Electrotonic Measurements by Electric Field-Induced Polarization in Neurons: Theory and Experimental Estimation

G. Svirskis,*# A. Baginskas,* J. Hounsgaard,# and A. Gutman*
*Laboratory of Neurophysiology, Biomedical Research Institute, Kaunas Medical Academy, 3000 Kaunas, Lithuania, and #Department of Medical Physiology, The Panum Institute, Copenhagen University, Copenhagen DK-2200, Denmark

ABSTRACT We present a theory for estimation of the dendritic electrotonic length constant and the membrane time constant from the transmembrane potential (TMP) induced by an applied electric field. The theory is adapted to morphologically defined neurons with homogeneous passive electric properties. Frequency characteristics and transients at the onset and offset of the DC field are considered. Two relations are useful for estimating the electrotonic parameters: 1) steady-state polarization *versus* the dendritic electrotonic length constant; 2) membrane time constant *versus* length constant. These relations are monotonic and may provide a unique estimate of the electrotonic parameters for 3D-reconstructed neurons. Equivalent tip-to-tip electrotonic length of the dendritic tree was estimated by measuring the equalization time of the field-induced TMP. For 11 turtle spinal motoneurons, the electrotonic length from tip to tip of the dendrites was in the range of 1–2.5 λ, whereas classical estimation using injection of current pulses gave an average dendrite length of 0.9–1.1 λ. For seven ventral horn interneurons, the estimates were 0.7–2.6 λ and 0.6–0.9 λ, respectively. The measurements of the field-induced polarization promise to be a useful addition to the conventional methods using microelectrode stimulation.

GLOSSARY

a	area of the cross section of the dendrite
A	amplitude of the harmonic response at the soma
D	representative apparent diameter of the dendrites of the cell
D_i	apparent diameter of the ith dendritic segment
E	electric field strength
g_s	admittance of soma membrane
H	characteristic duration of the transient
L	equivalent tip-to-tip length of the dendritic tree
L_d	average electrotonic length of the dendrites from soma
L_t	average electrotonic tip-to-tip length of the dendrites
R	specific membrane resistance
R_{in}	cell input resistance
s	total cell surface
s_i	fraction of the total cell surface, which is distal with respect to the center of the ith dendritic segment
s_s	soma surface
S	resistance of the impalement shunt
t	time
T	duration of the DC field pulse
u	extracellular potential
U	amplitude of the harmonic extracellular potential
v	intracellular potential
V	complex amplitude of the harmonic intracellular potential
w	transmembrane potential
w_s	soma transmembrane potential
w_{st}	steady soma transmembrane potential
w^0_{st}	steady soma transmembrane potential induced by a DC field of unit strength
W	complex amplitude of the harmonic transmembrane potential
W_s	complex amplitude of the harmonic transmembrane potential at the soma
x	axial coordinate of dendrite
X	length of the homogeneous dendritic segment
Z_{in}	complex input resistance
Z_{Li}	complex load resistance at the distal end of the ith dendritic segment

Greek symbols

α_i	angle between the ith dendritic segment and the field direction
β	direction of the DC field, which does not polarize the soma
θ	cyclic frequency
λ	electrotonic length constant of a dendrite with an apparent diameter of 1 μm
Λ	complex electrotonic length constant of a dendrite with an apparent diameter of 1 μm
μ	time delay of the soma transmembrane potential with respect to a slowly changing field
Π	perimeter of a dendrite with an apparent diameter of 1 μm
ρ	specific dendroplasmic resistance
τ	membrane time constant

Received for publication 3 February 1997 and in final form 21 August 1997.

Address reprint requests to Dr. A. Gutman, Laboratory of Neurophysiology, Kaunas Medical Academy, 9 Mickeviciaus St., 3000 Kaunas, Lithuania. Tel.: 370-7-204536; Fax: 370-7-220733; E-mail: arbagi@kma.Lt.

0006-3495/97/12/3004/12 $2.00

τ_1 first charge equalization time constant
φ phase shift of the harmonic transmembrane potential at the soma
ω characteristic resistance of a dendrite with an apparent diameter of 1 μm
Ω complex characteristic resistance of a dendrite with an apparent diameter of 1 μm

INTRODUCTION

The computing capacity of neurons depends on the electrotonic properties of dendrites. Only good knowledge of electrotonic structure allows one to understand the functional role of the interactions between synaptic and voltage-sensitive currents. Defining the ohmic features of dendrites is an urgent problem. Unfortunately, it is still difficult to solve this problem satisfactorily. For example, estimates of the electrotonic length of Purkinje cells differs 10 times (Chan et al., 1988; Rapp et al., 1994). In electrotonically long cells, even the membrane time constant τ, is not measured reliably, because the amplitude of the slowest exponential component of the potential transient, i.e., $\exp(-t/\tau)$, is small (Major et al., 1993). Additional difficulties arise from the complicated compensation of the access impedance (Jackson, 1992; Major, 1993; Spruston et al., 1994) and the possible impalement shunt (Durand, 1984; Kawato, 1984; Gola and Niel, 1993; Spielmann et al., 1993; Spruston et al., 1994). One needs to increase the number of unknown parameters when imitating the response of the cell to an electric stimulus. Measurements of membrane resistance in isolated cells by the whole-cell patch-clamp method are more reliable (Brown et al., 1993). These cells are electrotonically short; thus their large input resistance, R_{in}, is not influenced by the dendroplasma resistance and access parameters. R_{in} depends only on the membrane resistance. However, it is not certain whether an isolated neuron shares parameters with a normally functioning nerve cell.

At present, there is a single widely accepted procedure for determining the electrotonic structure of neurons, based on imitating the response to a short current pulse in a morphologically defined cell (Major et al., 1994). In this case four independent parameters of the supposedly homogeneous cell are chosen: the membrane capacitance (C), the impalement shunt (S), the specific membrane resistance (R), and the specific dendroplasmic resistance, ρ. Preference is given to whole-cell patch-clamp recordings, because in this case there is no impalement shunt (Major et al., 1994; but see also Thurbon et al., 1994). Nevertheless, three parameters are still too many for a unique imitation of the rather simple shape of the response to a current pulse. In addition, one must bear in mind that the very beginning of the response is contaminated by the capacitive current of the pipette (Major et al., 1994). The response to the current pulse is relatively insensitive to the distal membrane, because the effect of the sealed distal end is equivalent to a mirror current source that is twice as distant as the distal end is (Jack et al., 1975). The parameter values determined may be equivocal. For example, the calculated values for R differ by as much as 10 times in the same population of neurons (Thurbon et al., 1994).

Whole-cell patch-clamp data are complicated by possible wash-out from the cytoplasm of small organic molecules that may regulate membrane properties. Therefore, it is uncertain whether the electric properties of neurons are distorted by the experimental procedures (Edwards and Stern, 1991; Major et al., 1994). On the other hand, impalement by the sharp electrodes is not always accompanied by a shunt (Svirskis et al., 1997).Therefore, as the existing knowledge on passive electric parameters in neurons is unreliable, it is necessary to develop new approaches for measuring the electric parameters.

For the electrotonic measurements one may use the polarization of neurons induced by an applied electric field (Hounsgaard and Kiehn, 1993; Baginskas et al., 1993; Gutman and Svirskis, 1995). The stimulation by the electric field is particularly convenient because it provides a direct check of the assumption that the soma-dendritic membrane has homogeneous passive membrane properties (Svirskis et al., 1997). The field effect on the transmembrane potential (TMP) is equivalent to current sources at the distal ends of the dendrites. Thus the soma TMP is more sensitive to distal membrane than is the current-induced polarization. In tissue slices one may achieve homogeneity of the field (Andreasen and Nedergaard, 1996; Richardson and O'Reilly, 1995); thus the field-based methods seem practical. The electric field-based method is popular in electrotonic measurements of unbranched fibers (Trifonof and Chailakhian, 1975; Altman and Plonsey, 1989). It was also applied to the estimation of the electrotonic length of turtle Purkinje cells (Chan et al., 1988). (The cell was modeled as a homogeneous cylindrical cable without an injury shunt. By using intradendritic recording in many points, the authors estimated the Purkinje cell as 1.5–2 λ, length constant, long.)

Our aim is to demonstrate that measurements based on an applied electric field are promising for estimating the electrotonic structure of neurons. We assumed that an impalement shunt is absent, the membrane and cytoplasm are electrically homogeneous, and the shape of the cross section of dendrites is, on average, uniform on the scale $\ll\lambda$ (Alaburda and Gutman, 1996). In this case, the field-induced transmembrane potential depends only on the electrotonic length constant, λ, defined for some diameter and membrane time constant, τ. Of course, the method needs 3D reconstruction of the neuron. As independent electrodes are used for stimulation and recording, the compensation for the access impedance is not necessary.

The arguments above enable us to propose the field-based method as a promising complement to the already accepted methods for electrotonic measurements. Here we analyze a simplified case when the impalement shunt is absent. Thus the equations derived are primarily applicable to whole-cell recordings and to sharp-electrode recordings without an injury shunt (Svirskis et al., 1997).

We 1) present a general theory for field-induced soma TMP, 2) propose electrotonic measurements based on this

theory, and 3) estimate the average tip-to-tip electrotonic length of dendrites of motoneurons and ventral horn interneurons in turtle spinal cord by measuring the membrane time constant and equalization time of the field-induced TMP.

METHODS

Method substantiation

We must identify how the effects of an applied electric field depend on the electrotonic parameters. We assume that an impalement shunt is absent, and that the membrane and cytoplasm are electrically homogeneous. We will use a set of electrotonic parameters: membrane time constant, $\tau = RC$; electrotonic length constant, $\lambda = (Ra/\rho\Pi)^{1/2}$; and characteristic resistance, $\omega = (R\rho/a\Pi)^{1/2}$. The latter two parameters are defined for a homogeneous dendritic segment with an apparent diameter, $D = 1$ μm. Here a is the area of cross section of the cable and Π is the perimeter. The apparent diameter, D, is a morphologically measured quantity, $\Pi \approx D$ and $a \approx D^2$, with proportionality coefficients that are constant along the entire dendritic tree on the macroscopic scale $\ll\lambda$ (Alaburda and Gutman, 1996). Because each parameter from the electrotonic set has its own separate meaning for the physical phenomena, this set provides several advantages against the physical set R, ρ, C. For example, if only the electrotonic length constant λ for $D = 1$ μm is found, then by recalculating λ for each dendritic segment, the electrotonic structure of the dendritic tree can be defined, even in the absence of the estimation for R and ρ. The definition of the parameters from the physical set is restricted by the assumption that dendrites are cylindrical cables. If soma can be represented as a part of dendrites, there is no need to explicitly calculate values of R and C. Then for the electrotonic set, it is only important that the shape of the cross section along the entire dendritic tree is, on average, uniform on the macroscopic scale $\ll\lambda$ (Alaburda and Gutman, 1996).

Let us begin with the general cable equation for a homogeneous segment of an ohmic dendrite in an electric field:

$$D\lambda^2 \frac{\partial^2 v}{\partial x^2} = \tau \frac{\partial w}{\partial t} + w \tag{1a}$$

Here the term on the left is the derivative of the axial current, and v is the intracellular potential; the terms to the right define the transmembrane current. Transmembrane potential, $w = v - u$; u is the extracellular potential; x is the axial coordinate. To analyze the transients, we will use Fourier decomposition of the field and the transmembrane potential of the cell. If the field is harmonic, $u = U\exp(j\theta t)$, where θ is the cyclic frequency, and j is an imaginary unit, then the equation is simplified and acquires the form analogous to the equation for the stationary case, although the parameters become complex (Gutman, 1980; Tranchina and Nicholson, 1986):

$$D\Lambda^2 \frac{\partial^2 V}{\partial x^2} = W \tag{1b}$$

where the length constant for harmonic potentials $\Lambda = \lambda/(1 + j\theta t)^{1/2}$. V and W are complex amplitudes of the corresponding potentials. The boundary conditions at the points of break of the homogeneity (change of apparent diameter, branching, bending, and the end of dendritic branch) are the usual:

$$\sum_i \frac{dV_i}{dx_i} \cdot D_i^2 = 0 \tag{2}$$

The sum includes all segments that are connected to the given point.

The solution of Eqs. 1 and 2 depends on angles between the axis and the field, lengths, and the diameters of each segment, as well as on unknown parameters λ and τ. If the field is homogeneous, one may insert w instead of v in Eqs. 1a and 1b. The dependence on the field strength and orientation will remain only in the boundary conditions, Eq. 2 (Appendix A, Eq. A2b). Here we present the explicit expression of the complex amplitude for the soma transmembrane potential, $W_s(\theta)$, induced by a harmonic field (Appendix A):

$$W_s(\theta) = -E\frac{\Lambda}{\Omega} Z_{in} \sum_i \frac{D_i^2 \cos\alpha_i (1 - 1/(\cosh(X_i/\Lambda\sqrt{D_i}) + \Omega/D_i^{3/2} Z_{L_{ik}} \sinh(X_i/\Lambda\sqrt{D_i})))}{\prod_k (\cosh(X_{ik}/\Lambda\sqrt{D_{ik}}) + \Omega/D_{ik}^{3/2} Z_{L_{ik}} \sinh(X_{ik}/\Lambda\sqrt{D_{ik}}))} \tag{3}$$

Here X is the length of a homogeneous dendritic segment; E is the field strength; α is the angle between the segment and the field; Ω is the characteristic impedance, $\Omega = \omega/(1 + j\theta t)^{1/2}$, for the segment with $D = 1$ μm; Z_{in} is complex input resistance at the soma; Z_L is the complex load resistance at the distal end of the segment. The sum includes all dendritic segments of the cell; the product is carried out through the segments of the dendritic path, connecting the soma with the proximal end of the ith segment. It is evident that all Z_L and Z_{in} are proportional to Ω if there is no impalement-injury shunt. Thus $W_s(\theta)$ and $w_s(t)$ depend only on two nongeometrical parameters, λ and τ.

Equation 3 has an asymptotic limit (Gutman and Svirskis, 1995), derived in Appendix B:

$$W_s(\theta) = -\frac{E}{S} \cdot \sum_i X_i s_i \cos\alpha_i \tag{4a}$$

when the following inequality holds:

$$\lambda^2 D/\sqrt{1 + \theta^2\tau^2} \gg L^2 \tag{4b}$$

where s is the total surface of the neuron; s_i is its distal fraction with respect to the center of the ith segment; L is an equivalent tip-to-tip length of the dendritic tree. Here D is its representative apparent diameter.

It is evident that the asymptotic value is reached only when $\lambda \gg L$, because the increase in θ only weakens the inequality. As the asymptote of $W_s(\theta)$ does not depend on θ, Eq. 4a also defines the asymptote for the stationary response, $w_{st}(\lambda)$, to the field step. In the case of large λ, we can evaluate the characteristic time of the transient, H. The order of H is defined by the range of characteristic frequencies, $\theta \approx 1/H$, for which the response amplitude, $W_s(\theta)$, neither is vanishing nor has the asymptotic value of Eq. 4a. In this range of frequencies, approximate equality, $\lambda^2 D/\sqrt{1 + \theta^2\tau^2} \approx L^2$, holds. Finally, we get

$$\lambda\sqrt{D} \times \sqrt{H/\tau} \approx L \tag{4c}$$

Equation 4 is useful for analysis and control of the solutions presented below. Note that the characteristic time of the transient is decreasing when λ is increasing.

Calculation methods

Although Eq. 3 provides a complete analytical solution for the field-induced soma potential, but it is inconvenient for calculations. Our calculation algorithm is based on the superposition of the effects of the currents from the adjacent segments and the field.

The transmembrane potential at the proximal end of a homogeneous segment is defined by the input current and the field (Tranchina and Nicholson, 1986):

$$W(x, \theta) = -\left.\frac{dV}{dx}\right|_0 \cdot A(x, \Lambda) + E \cdot B(x, \Lambda) \tag{5}$$

The second term includes the field effect on this segment and the boundary condition at the distal end that reflects the field-induced polarization of

more distal dendrites. If the potential is induced only by the field, then (Appendix C)

$$W_s(\theta) = E\frac{\Lambda}{\Omega}\sum_i D_i^2\frac{B_i(\Lambda)}{A_i(\Lambda)}\Big/\left(\frac{\Lambda}{\Omega}\cdot\sum_i\frac{D_i^2}{A_i(\Lambda)} + g_s\right) \quad (6)$$

Here the admittance of the soma membrane, $g_s = s_s/(\Lambda \cdot \Omega \cdot \Pi)$; shunt is not considered; s_s is the soma surface; the sum includes the proximal segments of all dendrites. The definition of an algorithm for calculating the coefficients $A(\Lambda)$ and $B(\Lambda)$ is described in Appendix C.

It is obvious that all of the results in this section may be used for the stationary field. In this case one must change the complex parameters Λ, Ω, and various complex resistances for real λ, ω, and corresponding resistances.

General description of the calculations

We have calculated $w_s(t)$ at the onset and the offset of a DC field, during the harmonic field stimulus, and during a field ramp for two reconstructed nerve cells. These two neurons were chosen because of their different branching patterns: the hippocampal interneuron is very asymmetrical and has one long apical dendrite and several short basal dendrites (Fig. 1 *A*, *inset*), whereas the motoneuron has almost symmetrical dendritic branching (Fig. 1 *B*, *inset*).

The interneuron is from the stratum pyramidale of the CA1 field in the rat hippocampus (Thurbon et al., 1994). We have used the parameter values suggested for the neuron considered (Thurbon et al., 1994): $R = 14.4\ k\Omega \cdot cm^2$, $\rho = 410\ \Omega \cdot cm$, and $C = 1\ \mu F/cm^2$. Hence for a dendrite 1 μm in diameter, the length constant $\lambda = 296\ \mu m$ and the characteristic resistance $\omega = 1.547\ G\Omega$. The axon of this cell branches almost symmetrically with respect to the stratum pyramidale. The neuron has just four basal dendrites with limited branching. The field was oriented in the direction of the apical dendrites in the temporal plane. The contribution to the soma polarization of the symmetrical axon may be neglected (Gutman and Svirskis, 1995; Tranchina and Nicholson, 1986).

The motoneuron is from turtle spinal cord (Figure 2 *C* in Ruigrok et al., 1984). The diameters, D, of the dendritic branches were kept constant between branch points and were derived from the regression curve, $D = 0.55 + 0.53n\ \mu m$, where n is the number of the terminal branches emerging from a particular branch (Ruigrok et al., 1984). The smallest diameter was 1 μm. The electrotonic parameters chosen were $\tau = 20$ ms, $\lambda = 410\ \mu m$, $\omega = 1560\ M\Omega$, where λ and ω are calculated for a cable with a diameter of 1 μm. With these parameters, the input resistance for the model neuron and the characteristic time for the potential decay after a field step fell in the range of values observed experimentally (Svirskis et al., 1997; see Discussion also). The field was oriented in the lateral direction and was uniform. The axon was approximately perpendicular to the chosen field direction and therefore was not considered in the calculations.

The dendrites were divided into linear cylindrical segments. For each segment, its angle with respect to the field was determined. Calculations were accomplished by means of the Fourier transformation. For the DC

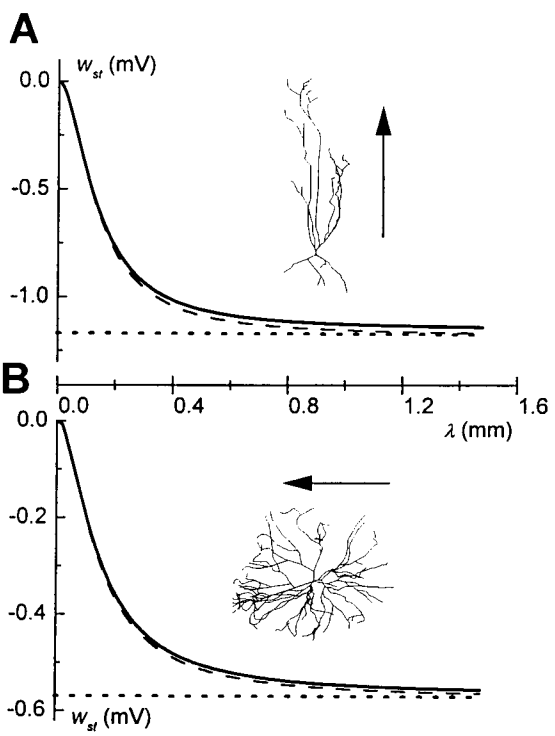

FIGURE 1 Dependence of steady soma polarization on λ (*solid line*). *Dashed lower curve*, All diameters increased by 0.1 μm; *dotted line*, asymptote when $\lambda \to \infty$. Here and below, except for specially noted cases, the DC field is 10 mV/mm strong. (*A*) The dependencies for the hippocampal interneuron. *Inset:* Computer-generated scheme of the neuron. Geometry, including orientation, of dendritic segments is defined according to 3D reconstruction (Thurbon et al., 1994). Arrow denotes the direction of the field. (*B*) The dependencies for the motoneuron of the turtle spinal cord. *Inset:* Computer-generated scheme of the cell. Geometry, including orientation, of dendritic segments is defined according to figure 2 of Ruigrok et al. (1984).

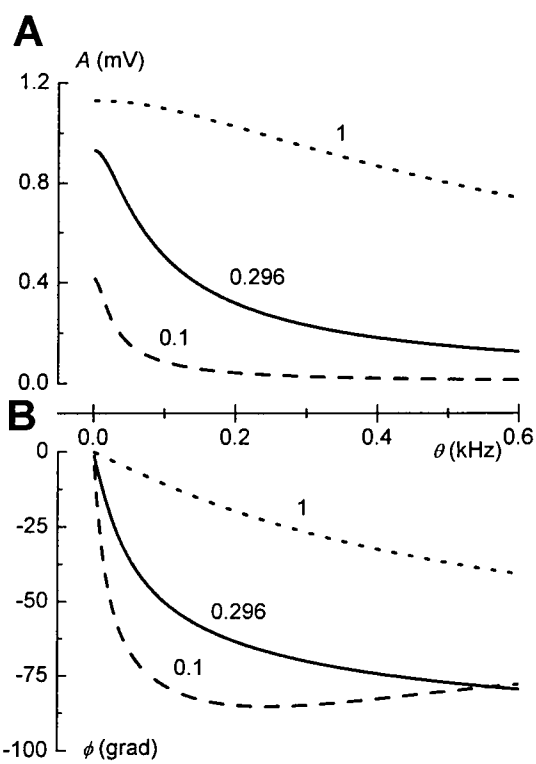

FIGURE 2 Frequency characteristics of the harmonic field-induced soma polarization in hippocampal interneuron. Field amplitude, 10 mV/mm. Abscissa, cyclical frequency θ. λ (mm) is written at the curves. $\tau = 14.4$ ms and $\lambda = 0.296$ mm, following the estimation of Thurbon et al. (1994) for the cell considered. (*A*) Amplitude. (*B*) Phase characteristics.

field pulse, the calculation formula derived in Appendix D is

$$w_s(t) = \begin{cases} \frac{2}{\pi}\int_0^\infty \mathrm{Re}(W_s(\theta))\frac{\sin(\theta t)}{\theta}\,d\theta, & 0 \le t \le T \\ \frac{2}{\pi}\int_0^\infty \mathrm{Re}(W_s(\theta))\frac{\sin(\theta t) - \sin(\theta(t-T))}{\theta}\,d\theta, & t \ge T \end{cases} \quad (7)$$

Here T is pulse duration. We test the results by means of compartmental calculations (Tranchina and Nicholson, 1986; Baginskas et al., 1993; Svirskis et al., 1997).

The same calculation methods were used with rising and declining field ramp (Appendix D).

Methods for the experimental procedures

Transverse sections of the lumbar spinal cord were obtained as described before (see Hounsgaard et al., 1988; and Svirskis et al., 1997) from turtles (*Pseudemys scripta elegans*). The bath medium contained (mM) 120 NaCl, 5 KCl, 15 $NaHCO_3$, 20 glucose, 2 $MgCl_2$, 3 $CaCl_2$. 6-Cyano-7-nitroquinoxaline-2,3-dione (CNQX) (40 μM) (Tocris Cookson, Bristol, England) was applied to block excitatory synaptic potentials.

For experiments a section of the cord, 1–2 mm thick, glued at the end to a piece of filter paper, was placed in the recording chamber between two silver chloride electrodes (see figure 2 *A* in Svirskis et al., 1997). The extracellular potential gradient in the tissue was 3–4 mV · mm^{-1} 50–200 mm below the surface of the tissue.

For recording field effects, sharp and patch electrodes were pulled from the borosilicate glass tubes with an outer diameter of 1.5 mm and an inner diameter of 0.86 mm. Sharp electrodes were filled with 1.5 M KCl and 0.5 M potassium acetate. Patch electrodes were filled with 125 mM potassium gluconate and 9 mM HEPES, and pH was adjusted to 7.4 with KOH. To reduce noise, 128 sweeps were averaged on a HIOKI digital oscilloscope (HIOKI E. E. Corp., Nagano, Japan) and fed to a computer for later analysis. After all measurements were accomplished, the electrode was withdrawn from the cell and the extracellular potential, induced by the same field step stimulus, was recorded, averaged, and subtracted from the intracellular potential to get the transmembrane potential. The electrotonic estimates were obtained from four motoneurons recorded with sharp electrodes, and seven motoneurons and seven interneurons recorded with patch electrodes. All responses to the field step were monotonic, indicating the homogeneity of passive membrane properties (Svirskis et al., 1997). There were no significant differences for the same type of cells between input resistance, time constant, and spike amplitude obtained with different recording techniques (Svirskis et al., 1997). For these reasons, no distinction was made when the data from motoneurons were analyzed.

The transients of the response to the field are very different from the response to the current injection through the microelectrode. The characteristic time of the field-induced transient in homogeneous neurons is much faster than τ (Svirskis et al., 1997). This property of the response to the field stimulation is due to the zero total charge induced on the membrane. The onset and offset of the DC field do not induce a net charge in homogeneous cells, because every line of the field crosses the membrane in both directions (Svirskis et al., 1997). Thus the slowest decay is analogous to Rall's first charge equalization time constant, τ_1 (Svirskis et al., 1997). The equalization of charges takes place between opposite ends of the dendritic tree of the neuron, where opposite charges are induced by the field. This makes the difference with current injection, where equalization takes place between soma and the distal dendrites. The transient of the response to the field step can be used for the estimation of the tip-to-tip electrotonic length, L_t, of the dendrites, using the classical equation (Rall, 1967; Rall et al., 1992)

$$L_t = \pi/\sqrt{\pi/\tau_1 - 1} \quad (8)$$

RESULTS

Theoretical results

Let us begin with the stationary polarization at the soma w_{st}. The stationary response to the field depends only on the electrotonic parameter λ. It approaches an asymptotic value defined by Eq. 4a as $\lambda \to \infty$ (Fig. 1). According to the criterion Eq. 4b, the soma polarization almost reaches the asymptotic value when $\lambda D^{1/2} \approx 2L$, as the cell becomes electrotonically compact. For the interneuron considered, $L \approx 0.3$ mm, $D \approx 2$ μm. Indeed, the asymptote is almost reached at $\lambda \approx 0.5$ mm (Fig. 1 *A*). Similar dependences $w_{st}(\lambda)$ were calculated for the turtle motoneuron (Fig. 1 *B*).

Next let us consider the frequency characteristics of the soma response to a harmonic field, $e^{j\theta t}$. The harmonic potential may be expressed in the form $w_s(t) = W_s(\theta)e^{j\theta t} = Ae^{j(\theta t+\varphi)}$. For the hippocampal interneuron (Thurbon et al., 1994), the dependences of the amplitude, A, and phase shift, φ, on the cyclic frequency, θ, are shown in Fig. 2. According to Eq. 3, these variables depend only on two parameters, λ and τ. Hence the amplitude and phase shift of the response to the harmonic field stimulus could be useful for the evaluation of electrotonic parameters.

To facilitate the comparison of results obtained using different stimulations, we shall introduce the new variable: the slope of the phase shift, $\mu = -d\varphi/d\theta$, when $\theta \to 0$. Because $W_s(\theta) \to A(0)e^{-j\theta\mu}$ when $\theta \to 0$, the parameter $A(0)$ is the stationary soma polarization w_{st} induced by the DC field, and μ is the time delay of the soma polarization with respect to a slowly changing field. In this context, one may define the field as slowly changing if, for all essential harmonic components of the response, $\varphi \approx -\mu\theta$ and $A(\theta) \approx A(0)$. The delay μ approaches 0 as $\lambda \to \infty$ (Fig. 3 *A*) because the field does not affect the intracellular potential in electrically compact cells, in this case, $w = -u$ (Gutman, 1980). Slow field ramps may be used to measure μ. If the field grows linearly in time, then $w_s(t)$ increases linearly as well after a certain transitional period. Let us consider $w_s(E)$ (see Appendix D). This curve becomes an asymptotic line, which differs from the stationary one, $w_s = Ew_{st}^0$, in the parallel shift $\Delta E = \mu\, dE/dt$ (Fig. 3 *B*). Here w_{st}^0 is the soma transmembrane potential, induced by a DC field of unit strength, $E = 1$. The shift corresponds to the change in the field during the delay μ. If the field rises and decreases linearly with the same speed, capacitive hysteresis with the width, $2\mu\, dE/dt$, is observed (Fig. 3 *B*). The application of the clamped current or potential ramp for the electrotonic measurements was considered previously (Butrimas and Gutman, 1980; Gutman, 1984). This method of measuring μ seems more suitable than the usual method of sinusoidal wave phase shift.

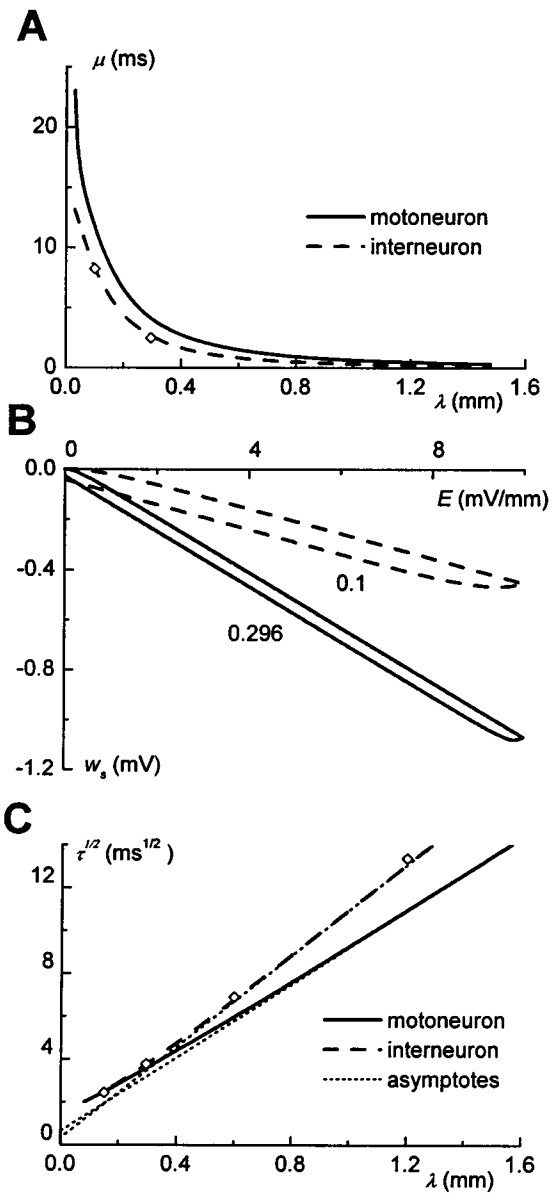

FIGURE 3 (*A*) Dependence of delay μ on λ for slow processes. *Solid line*, Motoneuron; *dashed line*, interneuron. (*B*) Hysteresis of soma potential-field dependence at field ramp up and down. The hysteresis is caused by membrane capacitance. The curves are calculated for two different λ values which (in mm) are indicated at the curves. The speed of the ramp was 0.1 mV/(mm · ms). (*C*) Dependence of τ on λ, obtained from delay μ (*A*) for slow processes (*solid line*, motoneuron; *dashed line*, interneuron) and from shape invariance of normalized transients at DC field switching (*diamonds*). In accordance with Eq. 4c, the curves for large λ approach asymptote $\tau \approx \lambda^2$ (*straight lines*). The ordinate τ is presented as $\tau^{1/2}$ to make the asymptote a straight line.

Because the response of the cell to the harmonic field depends only on λ and τ, the delay may be expressed as follows: $\mu = \tau f(\lambda)$. The function $f(\lambda)$ for the parameters of Thurbon et al. (1994) may be derived from Fig. 3 *A* if one divides the ordinate by $\tau = 14.4$ ms. Thus a set of λ and τ values corresponds to the measured value of μ. This set determines a function $\tau(\lambda) = \mu/f(\lambda)$ (Fig. 3 *C*). According to Eq. 4c, the transition time $H \approx \tau L^2/D\lambda^2$ when Eq. 4b holds; thus $\tau(\lambda)$ asymptotically becomes parabolic: $\tau \approx \lambda^2 DH/L^2$ (Fig. 3 *C*). The dependence $\tau(\lambda)$ converges to a parabola already when $\lambda > 0.5$ mm for both interneuron and motoneuron. The same dependence between λ and τ can be defined for the stimulation with a field step. At the onset and offset of the DC field, the transient $w_s(t)$ is monotonic for both cells: interneuron (Fig. 4 *A*) and motoneuron (not shown). The transient depends on τ and λ, although τ simply defines the scale of the time axis. Decay of the transients is much faster than the membrane discharge. The shape of the modeled transients may be used to estimate the parameters τ and λ by comparing them with real-time curves obtained experimentally. To compare the shapes, first let the amplitude for both the theoretical and the experimental transients be normalized to 1. Second, let us relate the time axes by changing the model time scales until curves intercept at the level $1/e$ (Fig. 4, *B* and *C*). We have performed this time and amplitude transformation for all modeled curves. In agreement with the relationship between λ and τ obtained for slow harmonics (Fig. 3 *C*), all normalized transients become almost identical for λ values when $\tau(\lambda)$ reaches the asymptote (Fig. 3 *C*). When the cell is not very compact electrotonically, the shapes are similar and deviations are small compared to the amplitude. Thus the parameters τ and λ define only the time and voltage scales of the transients, as the shape is virtually invariant. Therefore, an experimental transient can be matched by a set of modeled transients with different λ and τ defined by some function $\tau(\lambda)$. Diamonds in Fig. 3 *C* show the values of the function $\tau(\lambda)$ for the transients, whose shapes are transformed to be similar to the one calculated with the parameters of Thurbon et al. (1994). These values are almost identical to $\tau(\lambda)$ obtained from the time delay μ (Fig. 3 *C*).

In principle, additional information can be obtained by considering how polarization depends on the field direction. Obviously, the field effect in ohmic cells depends sinusoidally on the field direction at each moment in time (Eqs. 3 and 4). Therefore, there is a certain field orientation that does not polarize the soma. Of course, the orientation of the field that yields no steady polarization depends only on λ. Let us consider this field orientation β in the temporal plane for hippocampal interneuron, where β is the angle between the field and the temporal projection of the apical dendrite. In our calculations β changes by only 5° as λ increases from 50 to 300 μm (not shown). The field orientation changes insignificantly as $\lambda > 300$ or < 50 μm. Thus, for the cell considered, the β value is not informative in electrotonic measurements. Moreover, β depends on the electrode position inside soma. Nevertheless, measuring β may serve as a means of control of the model and consistency of the reconstruction. When the steady soma polarization is small, the transients may no longer be monotonic. This happens because of the relatively large contribution of the basal dendrites and proximal oblique apical branches. We have considered this phenomenon (not shown). The transient reaches only 40 μV when there is no steady polarization. Its decay time

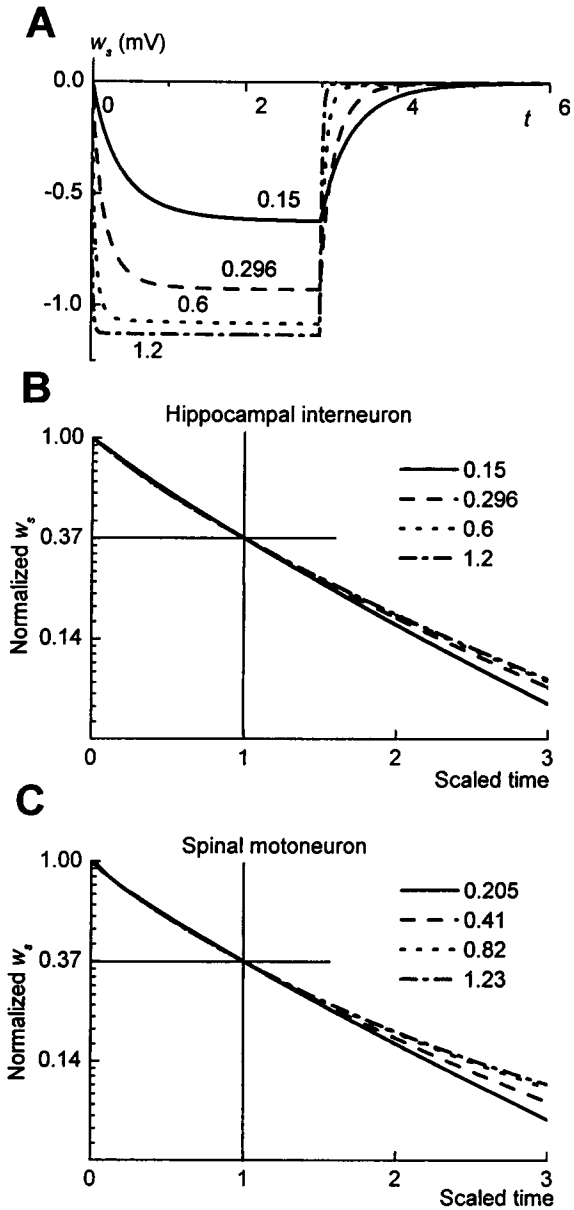

FIGURE 4 (*A*) Transients of hippocampal interneuron at the onset and offset of the DC field. The values of λ (in mm) are indicated at the curves. The field is switched on at the moment $t = 0$ and off at the moment $t = 3\tau$. (*B*) Normalized transients of the hippocampal interneuron at the offset of the field. All amplitudes are normalized to 1, and time scales are linearly transformed in such a way that all curves cross at the value $1/e$. The transient for $\lambda = 0.296$ mm decays to this level at the moment of 2.15 ms. *Note:* Curves for $\lambda = 0.296$, 0.6, and 1.2 mm almost merge. (*C*) Normalized transients of the spinal motoneuron at the offset of the field. For *B* and *C*, normalized potential is in logarithmic scale; λ values (in mm) are indicated in the legends.

constant $\approx \tau/3$. The nonmonotonic decay disappears for angles larger than $\beta \pm 5°$. Therefore, the nonmonotonicity of the homogeneous cell transients may be neglected in the analysis of experimental data. Possible impalement shunt and other membrane inhomogeneities may cause stronger and longer-lasting nonmonotonicity of the transients apparent in all field directions (Svirskis et al., 1997).

Thus the comparison between measured and theoretical field-induced soma polarization produces monotonic dependencies that may be useful for estimating the electrotonic parameters. They supplement the existing methods for the electrotonic measurements based on the imitation of the cell response to a brief current pulse. The combination of dependencies established above with the existing methods can increase the reliability of the estimation of parameters.

Experimental results

When full reconstruction of the neuron is not available, the field stimulation can be used for the estimation of the electrotonic length of the dendrites. We recorded the response to a current impulse (Fig. 5, *A* and *B*) and field step (Fig. 5 *C*) in turtle motoneurons and ventral horn interneurons. The responses to the field step were monotonic, indicating homogeneity of the passive properties of soma-dendritic membrane and the absence of a shunt (Svirskis et al., 1997). In the case of field stimulation, we can get the estimation of the average electrotonic distance, L_t, from tip to tip of the dendrites. According to Rall's classical formula (Eq. 8) and using the data presented in Fig. 5, the average electrotonic length of the dendrites $L_d = 0.9$ and $L_t = 1.3$ for the current and field stimulation, respectively. For the population of 11 motoneurons recorded, L_d ranged from 0.85 to 1.1 λ (1.0 ± 0.1) and L_t ranged from 1 to 2.4 λ (1.4 ± 0.4). For the seven interneurons, the same estimation gave L_d in the range of 0.6–0.9 λ (0.76 ± 0.04) and L_t in the range of 0.7–2.6 λ (1.6 ± 0.2). Spinal cord neurons have relatively symmetrical dendritic arbors (Ruigrok et al., 1984; Hounsgaard and Kjaerulff, 1992); thus $L_t \approx 2L_d$. Because the transmembrane potential induced by the electric field is largest in the direction of the field applied, the estimation of the electrotonic length is dependent on this direction. However, the estimation probably was not biased toward the shorter values, because turtle spinal cord motoneurons have their physically longest dendrites in the lateral direction (Ruigrok et al., 1985), which was used for the field application.

DISCUSSION

We have considered how the response to an applied field depends on the electrotonic parameters in 3D morphologically defined neurons. We used an electrotonic set of parameters: membrane time constant, τ; electrotonic length constant, λ; and characteristic resistance, ω; defined for the dendritic segment with an apparent diameter of 1 μm.

There are interrelated primary functions of frequency or time: the amplitude $A(\theta)$ and phase $\varphi(\theta)$ frequency characteristics (Fig. 2) and the transients at the onset and offset of the DC field (Fig. 4). These functions depend on the electrotonic parameters λ and τ that are being sought. Two useful relations were derived from the primary functions above. These relations are the dependence of stationary

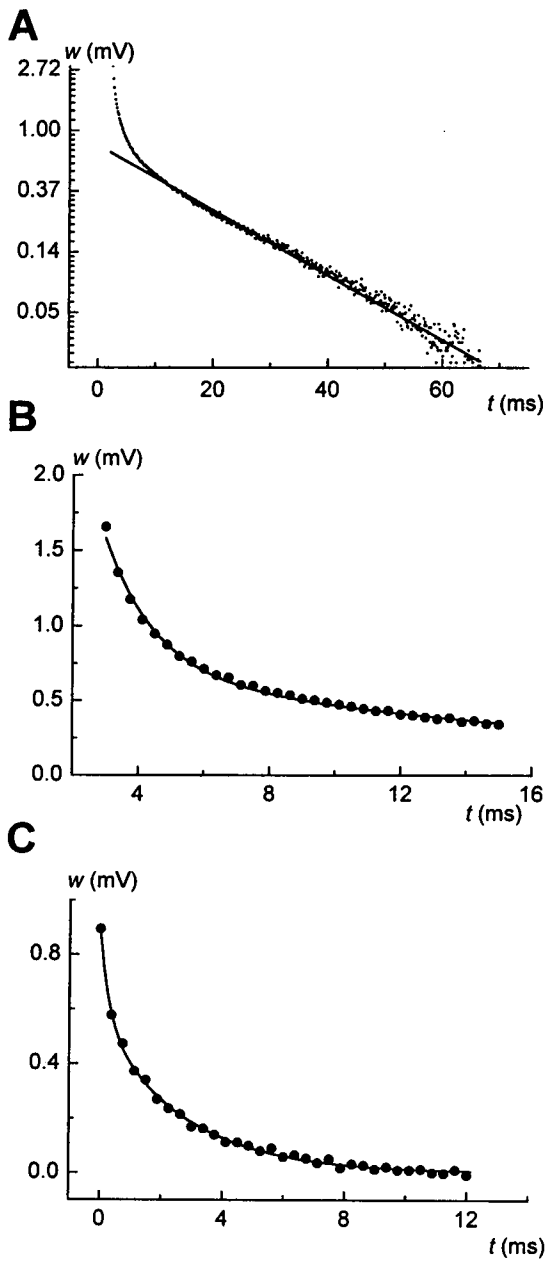

FIGURE 5 Experimental data for turtle motoneuron. (*A*) *Dotted line*, Response to brief current pulse; *straight line*, single exponential (τ = 19 ms) fitted to the late part of the response. Pulse duration, 1 ms. The potential is in logarithmic scale. (*B*) Early part of the response to the current pulse (*circles*). *Solid line*, Fitted double exponential (τ = 19 ms, τ_1 = 1.5 ms). (*C*) Transient of transmembrane potential at the offset of the field step (*circles*). *Solid line*, Fitted double exponential (τ_1 = 2.7 ms, τ_2 = 0.3 ms).

response to the field on λ, $w_{st}(\lambda)$ (Fig. 1), and the relation $\tau(\lambda)$ obtained from the phase shift of the slow harmonics of the response, or from the response to the field ramp (Fig. 3 *B*), or from the shape of the transients at the onset and offset of the DC field (Fig. 4). The third electrotonic parameter, characteristic resistance ω, could be found easily from the measurements of R_{in} if λ is already defined.

These relations could serve for robust estimation of the electrotonic parameters in neurons with very different electrotonic length. In electrotonically long cells ($L_t > 2$) like neocortical pyramidal cells (Larkman et al., 1992), the measurement of τ could be unreliable when stimulating with the current pulse injection. In this case the stationary response to the field, $w_{st}(\lambda)$, is very sensitive to the electrotonic length constant, λ (Fig. 1). After definition of λ from $w_{st}(\lambda)$, the membrane time constant, τ, can be found from the relation $\tau(\lambda)$. The ramp field stimulation may be used as a check. If the hysteresis (Fig. 3 *B*) is too narrow to be measured, this would mean that λ is very large and/or τ very small. In cells that are not very long electrotonically ($L_t <$ 2), like Purkinje cells (Rapp et al., 1994; Chan et al., 1988), hippocampal neurons (Major et al., 1994; Thurbon et al., 1994), and turtle motoneurons, τ can be measured directly (Fig. 5 *A*). Because $w_{st}(\lambda)$ may be less sensitive to λ, the electrotonic length constant could be defined also from the relation $\tau(\lambda)$. Because in both cases the dependencies involve no more than two parameters, the field-based methods make the estimation of the electrotonic structure more reliable than when only the current-injection-based methods are used.

The noise-related error should not be reduced by increasing the strength of the field, because too large w influences voltage-sensitive ion channels and may evoke nonlinear electrical phenomena. This error is better compensated for by averaging. Discrepancies from an ohmic response induced by strong fields are especially dangerous in relation to distal dendrites, where the polarization is greater than in the soma. For a cell like the hippocampal interneuron considered, one should limit w_s to $\pm$2 mV. For the interneuron we consider, this corresponds to polarization of the distal apical branches by $\sim\pm$5 mV. When averaging is used, the noise level could be reduced to 20 μV (Svirskis et al., 1997), which is equivalent to 2% of the response. An error of 2% causes a 7% error in λ, as evaluated from the stationary response of hippocampal interneuron to the field, when λ value is ~0.3 mm (Fig. 1 *A*).

The accuracy of the measured dendritic diameters is limited by the resolving power of the microscope. This error must be considered as well. The effect of an error in the measurement of the diameter is demonstrated in Fig. 1. If all segment diameters differ by 0.1 μm, then the error of λ is important and equals 30 μm for λ = 300 μm (Fig. 1 *A*). In fact, this error of λ is not very essential for the estimation of the electrotonic structure of the neuron. If the diameters are underestimated, then the calculated λ will be overestimated. These two errors partly compensate for each other when the electrotonic length of the dendrites is calculated. We calculated the overall electrotonic length of the cell with dendrites thinner by 0.1 μm. Despite a rise in λ by 10%, the electrotonic length decreased by only 2%.

The error caused by the influence of the axon on the field-induced soma polarization is of principal importance (Gutman and Svirskis, 1995; Svirskis et. al., 1997; Tranchina and Nicholson, 1986). In the case of the hippocampal interneuron considered, this influence on w_{st} is

small because of the symmetrical branching of the axon with respect to the recording site. The center of the whole axon "cloud" is positioned ~20 μm down the soma. For the field used in the calculations, the corresponding extracellular potential difference equals 0.2 mV. This difference would cause 0.1-mV polarization at the ends of a short, symmetrical cable. Its magnitude is much larger than the real influence of the axon for two reasons. First, the soma-dendritic impedance is very small in comparison to the axonal impedance (usually the latter is neglected when the cell impedance is calculated); thus the influence of the axon is almost short-circuited (Gutman, 1980; Tranchina and Nicholson, 1986). Second, the axon predominantly projects in a plane perpendicular to the field. Therefore, the long, nonpolarized branches shunt the polarization in the field-oriented short branches. Thus the influence of the axon is much less than 0.1 mV, and it could not change the estimation of λ too much for the hippocampal interneuron considered. However, because of long axon branches in the saggittal plane (Thurbon et al., 1994), the influence of the axon may distort the value of the angle β for the direction of the DC field, which does not polarize the soma. In the case of the turtle motoneuron the effect of the axon is small (Svirskis et al., 1997). The influence of an axon on polarization of the turtle Purkinje cell is small in radial fields, as the axon is nearly perpendicular to the dendrites (Chan et al., 1988). Certainly, it is more favorable to measure electrotonic parameters by means of a field-induced polarization in neurons with cut axons, like those in the cerebellar slices in the experiments of Rapp et al. (1994).

An inherent error in the present method is related to the inaccuracy in measurement of the extracellular potential. We measured it after withdrawing the patch electrode <20 μm from the cell. We cannot exclude the displacement of a few microns of the electrode along the field during the withdrawal or tissue deformation during the experiment. Thus an error of few tens of microvolts is inevitable.

An additional source of error in comparing calculations and measurements is the shunt, which may be induced by the recording electrodes. In the case of a considerable shunt, the cell response at the onset and offset of the DC field has a distinct over- and undershoot pattern (Svirskis et al., 1997). The steady soma potential $w_{st} = w_0/(1 + R_{in}/S)$ (Svirskis et al., 1997), where w_0 is the steady soma potential in the absence of a shunt, and R_{in} is the "true" input resistance of the cell without shunt S. For the hippocampal interneuron analyzed, R_{in} is evaluated from the response to the short current pulse and is equal to 125 MΩ (Thurbon et al., 1994). Subsequently, a gigaseal of 10 GΩ, which is common in good whole-cell recordings, may result in a relative mistake of ~1%. Obviously, the shunt may be considerably larger. If so, over- and undershoots are seen.

If it is difficult to avoid potential-dependent currents in a cell, the response to a brief field pulse can be used. The corresponding responses, $w_s(t)$ (not shown), are similar to the derivative of the transient at the onset of a DC field. The comparison of the shapes of the responses can give the function $\tau(\lambda)$, as described above (Fig. 3 *C*). The comparison procedure is identical to that proposed for the transients at the onset and offset of the DC field. The response to a brief pulse of the field does not carry any new information in comparison with the steady polarization value and the shape of the transient of the response to the field step. However, it may be more useful in practice because of the smaller influence of voltage- and time-dependent ionic currents.

The homogeneity of the field is an important condition for the proper evaluation of electrotonic parameters. In the experiments presented, the field strength varied by <15% along the whole dendritic tree. This error is particularly bad for the measurement of the stationary effect in almost symmetrical cells. However, such nonuniformity has little influence on the time course of the transient used for the estimation of the electrotonic length.

In the case of current pulse injection, estimation of the electrotonic length by using equalization time was shown to be unreliable (Rall et al., 1992). We tried to evaluate the method using equalization time of the field-induced TMP. In a model motoneuron (Fig. 1 *B*, *inset*) we applied the same procedures of estimation of electrotonic length as in experiments. The calculated transients were fitted with double exponentials: $C\exp(-t/\tau) + C_1\exp(-t/\tau_1)$ for a current pulse stimulus, and $C_1\exp(-t/\tau_1) + C_2\exp(-t/\tau_2)$ for a field step stimulus. Electrotonic lengths were estimated using Eq. 8. The calculations were done for three λ values: 300, 410, and 820 μm. The estimated electrotonic lengths, L_d, in the case of current pulse were 1.3, 1.0, and 0.7, respectively. In the case of the field step the estimated lengths, L_t, were the same when using τ_1 or τ_2 and equaled 1.9, 1.7, and 1.2. According to the experimental evaluation where $L_d = 1.0 \pm 0.1$ and $L_t = 1.4 \pm 0.4$, a λ value of 410 μm could serve as a representative result. In the model motoneuron for $\lambda = 410$ μm, most of the dendrites terminated at the electrotonic distance of 0.6–1.1 λ, with the longest branch reaching 1.5 λ. This means that the representative electrotonic tip-to-tip distance was 1.2–2.2 λ, which could explain the estimated length of 1.7 λ. However, in the case of smaller λ, the evaluation using field step underestimated tip-to-tip electrotonic length.

In conclusion, in addition to the existing methods for determining the electrotonic structure of morphologically defined homogeneous neurons, we propose the application of electric field-induced soma polarization. It is more sensitive to the distal membrane and depends only on τ and λ. The theory of the method provides two monotonic relations that can be used for a unique estimation of the electrotonic parameters. The tip-to-tip electrotonic length of the dendritic tree of turtle motoneurons was estimated from the experimental transients after the field step.

APPENDIX A

We shall express the field potential in a form that enables one to easily superimpose effects of separate dendritic compartments:

$$U = \begin{cases} 0, & x \le 0 \\ -Ex \cdot \cos\alpha, & 0 \le x \le X \\ -EX \cdot \cos\alpha, & x \ge X \end{cases} \quad \text{(A1)}$$

The boundary conditions for a cylindrical segment may be detailed as follows:

$$\left.\frac{dV}{dx}\right|_0 \cdot \frac{D^2\Lambda}{\Omega} = \frac{V(0)}{Z_{L0}}, \quad \text{(A2a)}$$

$$\left.\frac{dV}{dx}\right|_x \cdot \frac{D^2\Lambda}{\Omega} = -\frac{V(X) + EX\cos\alpha}{Z_L}. \quad \text{(A2b)}$$

Here $x = 0$ corresponds to the proximal and $x = X$ to the distal end; Z_{L0} is the load at the proximal and Z_L the load at the distal end. The general solution of Eq. 1b is

$$V(x) = -Ex\cos\alpha + V(0)\left(\cosh\left(\frac{x}{\Lambda\sqrt{D}}\right) + A\sinh\left(\frac{x}{\Lambda\sqrt{D}}\right)\right) \quad \text{(A3a)}$$

Let us insert it into the boundary conditions of Eq. A2. After rearrangement we have

$$V(0) = -\frac{Z_{in}ED^2\Lambda}{\Omega}\cos\alpha\left(1 - 1\Big/\left(\cosh\left(\frac{X}{\Lambda\sqrt{D}}\right) + \frac{\Omega}{D^{3/2}Z_L}\sinh\left(\frac{X}{\Lambda\sqrt{D}}\right)\right)\right) \quad \text{(A3b)}$$

where Z_{in} is the input impedance at the proximal end. The solution Eq. A3b means that the effect on the cell of the field distal to the point $x = 0$ is equivalent to the injection of current at this point. The expression at the right of Eq. A3b, except Z_{in}, describes the magnitude of this current. According to coupling symmetry (Carnevale and Johnston, 1982; Gutman, 1984), this current induces a potential in the soma that is equal to the potential at the point $x = 0$ induced by the same current through the soma membrane. To describe the effect of the whole field, one should 1) calculate the potential decay from the soma to the point $x = 0$ and 2) sum up the effects of all compartments. This results in Eq. 3, where 1) yields the product in the denominator.

APPENDIX B

The Λ modulus is

$$|\Lambda| = |\lambda/\sqrt{1 + j\theta\tau}| = \left|\frac{\lambda\sqrt{2}}{\sqrt{1 + \sqrt{1 + \theta^2\tau^2}} + j\sqrt{-1 + \sqrt{1 + \theta^2\tau^2}}}\right| = \frac{\lambda}{\sqrt[4]{1 + \theta^2\tau^2}} \quad \text{(B1)}$$

If $|\Lambda|$ is large enough, the values of *cosh* and *sinh* in Eq. 3 approach their polynomial values, $1 + X^2/2\Lambda^2D + X^4/24\Lambda^4D^2$ and $X/\Lambda D^{1/2} + X^3/6\Lambda^3D^{3/2}$, respectively. Retaining only the first small term in every sequence, we obtain the following:

$$W_s(\theta) = E\frac{\Lambda}{\Omega}Z_{in}\sum_i D_i^2\cos\alpha_i \times \frac{(1 + X_i^2/12\Lambda^2D_i)X_i^2/2\Lambda^2D_i + (1 + X_i^2/6\Lambda^2D_i)\Omega/D_i^{3/2}Z_{L_i} \times X_i/\Lambda\sqrt{D_i}}{1 + X_i^2/2\Lambda^2D_i + \Omega/D_i^{3/2}Z_{L_i} \times X_i/\Lambda\sqrt{D_i}} \times \frac{1}{1 + \sum_k (X_{ik}^2/2\Lambda^2D_{ik} + \Omega/D_i^{3/2}Z_{L_{ik}} \times X_{ik}/\Lambda\sqrt{D_{ik}})} \quad \text{(B2)}$$

In this case, one may express the input impedance of the cell as membrane impedance divided by the cell surface, $Z_{in} = \Omega\Lambda\Pi/s$, where Π is the perimeter of the dendrite of apparent unit diameter, and s is the total cell surface. Correspondingly, a load impedance, $Z_{L_i} = \Omega\Lambda\Pi/s_{L_i}$, where s_{L_i} is a proportion of the total cell surface that is distal with respect to the distal end of the ith dendritic segment. Only the second-order small terms exist in the above approximation, because factors at all *sinh* in Eq. 3 are proportional to $X/\Lambda D^{1/2}$. The sum in the denominator is taken over segments in the path, which connects the soma with the proximal end of the ith segment. Inserting these expressions into Eq. B2, after rearrangements we obtain

$$W_s(\theta) = -E\Big/s \times \sum_i X_i\left(\frac{X_i\Pi D_i}{2} + s_{L_i} + \frac{X_i^2}{6D_i\Lambda^2}\left(\frac{X_i\Pi D_i}{4} + s_{L_i}\right)\right) \cos\alpha_i\Big/\left(1 + \frac{X_i^2}{2\Lambda^2D_i} + \frac{X_i s_{L_i}}{\Lambda^2\Pi D_i^2}\right)\left(1 + \sum_k\left(\frac{X_{ik}^2}{2\Lambda^2D_{ik}} + \frac{X_{ik}s_{L_{ik}}}{\Lambda^2\Pi D_{ik}^2}\right)\right) \quad \text{(B3)}$$

Neglecting the small terms, and noting that $X_i\Pi D_i/2 + s_{L_i} = s_i$, where s_i is part of the total cell surface, which is distal with respect to the center of the ith dendritic segment, we simplify Eq. B3 to the asymptotic Eq. 4a. If the whole dendrite is represented as a homogeneous cable, then X and D are the representative length and diameter of the apical dendrite. Now the criterion of the asymptotic approximation is reduced to Eq. 4b.

APPENDIX C

Solving the boundary problem of fixed axial current at the ends of the segment in a homogeneous field, one gets the relationships between the potentials and their derivatives at both ends:

$$W(0) = \Lambda\sqrt{D}\frac{dW/dx|_X - dW/dx|_0\cosh(X/\Lambda\sqrt{D})}{\sinh(X/\Lambda\sqrt{D})} \quad \text{(C1a)}$$

$$W(X) = \Lambda\sqrt{D}\frac{dW/dx|_X\cosh(X/\Lambda\sqrt{D}) - dW/dx|_0}{\sinh(X/\Lambda\sqrt{D})} \quad \text{(C1b)}$$

Taking Eqs. 2 and A2 into account and the general solution in the form of Eq. 5, we express the derivative:

$$\left.\frac{dW}{dx}\right|_x = -W(X)\sum_m\frac{D_m^2}{A_mD^2} + E\left[\cos\alpha + \sum_m\frac{D_m^2}{A_mD^2}B_m\right] = -W(X)G + EF \quad \text{(C2)}$$

For terminal segments, $G = 0$, $F = \cos\alpha$. The sum is carried out for segments adjacent to the distal end of the considered segment, D_m are the diameters of adjacent segments, and D are the diameters of the considered more proximal segment. Equation C2 is also applied for the cases of the

diameter change inside a branch, when there is no summation. Inserting Eq. C2 in Eq. C1, a relationship between $W(0)$ and $dW/dx(0)$ is obtained. Replacing in this relationship dW/dx with $dV/dx + E\cos\alpha$ and comparing it with Eq. 5, one obtains the coefficients A and B, which are introduced in Eq. 5:

$$A = \Lambda\sqrt{D}\,\frac{\cosh(X/\Lambda\sqrt{D}) + \Lambda G\sqrt{D}\sinh(X/\Lambda\sqrt{D})}{\sinh(X/\Lambda\sqrt{D}) + \Lambda G\sqrt{D}\cosh(X/\Lambda\sqrt{D})} \tag{C3a}$$

$$B = \Lambda\sqrt{D}\,\frac{F}{\sinh(X/\Lambda\sqrt{D}) + \Lambda G\sqrt{D}\cosh(X/\Lambda\sqrt{D})} - A\cos\alpha \tag{C3b}$$

Starting the calculation from terminal segments, we finally find A and B for the proximal segment of every dendrite emerging from the soma. Using Eq. 5, one calculates the transmembrane potential at the soma:

$$W_s(\theta)\,\frac{\Lambda}{\Omega}\sum_n \frac{D_n^2}{A_n(\Lambda)} = \frac{\Lambda}{\Omega}\sum_n\left(ED_n^2\,\frac{B_n(\Lambda)}{A_n(\Lambda)} - D_n^2\left.\frac{dV}{dx}\right|_n\right) \tag{C4a}$$

The sum includes the proximal segments of all dendrites, and $dV/dx|_n$ is the axial gradient of the intracellular potential at the beginning of the nth dendrite. Let us add soma transmembrane current, $g_s W_s(\theta)$, to both sides of Eq. C4a, where g_s is the soma membrane admittance. Then

$$W_s(\theta) = \frac{I_c(\theta) + E\,\Lambda/\Omega\sum_n D_n^2\,B_n(\Lambda)/A_n(\Lambda)}{g_s + \Lambda/\Omega\sum_n D_n^2/A_n(\Lambda)} \tag{C4b}$$

Here $I_c(\theta)$ is the component of the current injected through the microelectrode, and the expression $D_n^2(\Lambda/\Omega)$ stands for the axial resistance of the proximal dendritic segment. Equation 6 follows from this if the potential is induced only by the field, $I_c = 0$.

APPENDIX D

We express the pulse of a DC field, $-T/2 \le t \le T/2$, as a series of cosines:

$$E(t) = \frac{1}{\pi}\int_0^{+\infty}(\exp(j\theta t) + \exp(-j\theta t))\,\frac{\sin(\theta T/2)}{\theta}\,d\theta = \frac{1}{\pi}\int_{-\infty}^{+\infty}\exp(j\theta t)\,\frac{\sin(\theta T/2)}{\theta}\,d\theta \tag{D1}$$

As cosines are a sum of two harmonic exponentials, we apply the procedure of cable reaction to a harmonic field (Eq. 6). The result is complex amplitude $W_s(\theta)$, and the polarization sought acquires the following form:

$$w_s(t) = \frac{1}{\pi}\int_{-\infty}^{+\infty}(\mathrm{Re}(W_s(\theta))\exp(j\theta t) + j\mathrm{Im}(W_s(\theta))\exp(j\theta t))\,\frac{\sin(\theta T/2)}{\theta}\,d\theta = \frac{1}{\pi}\int_{-\infty}^{+\infty}\mathrm{Re}(W_s(\theta))\cos(\theta t)\,\frac{\sin(\theta T/2)}{\theta}\,d\theta - \frac{1}{\pi}\int_{-\infty}^{+\infty}\mathrm{Im}(W_s(\theta))\sin(\theta t)\,\frac{\sin(\theta T/2)}{\theta}\,d\theta \tag{D2}$$

Equation D2 is derived according to the evenness of real and unevenness of imaginary components of $W_s(\theta)$. The principle of causality states that in physical systems $w_s(t) = 0$ for $t < -T/2$. This means that integrals of Eq. D2 are mutually equal at $t < -T/2$. This equality may serve as a test of the correctness of the calculations. Because of this equality and the obvious symmetry of these integrals with respect to t and θ, and after shifting the initial point of time with respect to the beginning of the pulse, one obtains

$$w_s(t) = \frac{4}{\pi}\int_0^{+\infty}\mathrm{Re}(W_s(\theta))\cos(\theta(t - T/2))\,\frac{\sin(\theta T/2)}{\theta}\,d\theta, \quad t \ge T \tag{D3}$$

Equation D3 can be used for the time moments during the field pulse. For this purpose, in accordance with the causality principle, one should put $T = t$ in Eq. D3, where t is the time from the beginning of the pulse. The sought-for Eq. 7 is achieved by elementary rearrangements.

Using analogous reasoning, we express $w_s(t)$ during field ramp:

$$w_s(t) = \frac{4}{\pi}k\int_0^{+\infty}\mathrm{Re}(W_s(\theta))\,\frac{\sin^2(\theta t/2)}{\theta^2}\,d\theta, \quad t \ge 0,\ E = kt \tag{D4a}$$

Inserting $\eta = \theta t/2$, we obtain

$$w_s(E) = \frac{2}{\pi}E\int_0^{\infty}\mathrm{Re}(W_s(2\eta/t))\,\frac{\sin^2(\eta)}{\eta^2}\,d\eta, \quad t \ge 0 \tag{D4b}$$

If the values of t are large enough and, thus, small θ dominates, one may insert into Eq. D4a only linear segments of amplitude and phase frequency characteristics, as $\theta \to 0$ (Fig. 1):

$$\mathrm{Re}(W_s(\theta)) \to w_{st}^0 \cdot \cos\mu\theta,\ \theta \to 0 \tag{D5a}$$

In this case, Eq. D4a simplifies to

$$w_s(E(t = a)) \to w_{st}^0 \cdot E(t = a - \mu),\ t \to \infty \tag{D5b}$$

In other words, ramp-induced transmembrane potential asymptotically approaches the steady polarization value, but this value is delayed by time μ.

We thank Jens Midtgaard (Copenhagen University) for collaboration and discussion. We are grateful to Jurate Andrulioniene and Aleksandras Gutmanas for their help with the English text.

We acknowledge grant LHH100 of the Lithuanian government and the International Science Foundation, and support of the Lithuanian Ministry of Science and Education. The experimental work was supported by the Danish MRC, the Lundbeck Foundation, and the Novo-Nordisk Foundation.

REFERENCES

Alaburda, A., and A. Gutman. 1996. Theory of cable with an irregular cross-section. *Biophysics.* 41:727–732 (translation from *Biofizika*).

Altman, K. W., and R. Plonsey. 1989. Analysis of the longitudinal and radial resistivity measurements of the nerve trunk. *Ann. Biomed. Eng.* 17:313–324.

Andreasen, M., and S. Nedergaard. 1996. Dendritic electrogenesis in rat hippocampal CA1 pyramidal neurons: functional aspects of Na^+ and Ca^{2+} currents in apical dendrites. *Hippocampus* 6:79–95.

Baginskas, A., A. Gutman, and G. Svirskis. 1993. Bi-stable dendrite in constant electric field: a model analysis. *Neuroscience.* 53:595–603.

Brown, A. M., P. C. Schwindt, and W. E. Crill. 1993. Voltage dependence and activation kinetics of pharmacologically defined components of the high-threshold calcium current in rat neocortical neurons. *J. Neurophysiol.* 70:1530–1543.

Butrimas, P., and A. Gutman. 1980. Theoretical voltage-current characteristic of the neurone input with even shift in the clamped potential of the soma. *RC*-dendrites. *Biophysics.* 25:1105–1109 (translation from *Biofizika*).

Carnevale, N. T., and D. Johnston. 1982. Electrophysiological characterization of remote chemical synapses. *J. Neurophysiol.* 470:606–621.

Chan, C. Y., J. Hounsgaard, and C. Nicholson. 1988. Effects of electric fields on transmembrane potential and excitability of turtle cerebellar Purkinje cells in vitro. *J. Physiol. (Lond.).* 402:751–771.

Durand, D. 1984. The somatic shunt cable model for neurons. *Biophys. J.* 46:645–653.

Edwards, F. A., and P. Stern. 1991. Amino acid-mediated EPSCs. *In* Excitatory Amino Acids and Synaptic Function. Academic Press, London. 171–195.

Gola, M., and J. P. Niel. 1993. Electrical and integrative properties of rabbit sympathetic neurones re-evaluated by patch clamping non-dissociated cells. *J. Physiol. (Lond.).* 460:327–349.

Gutman, A. 1980. Biophysics of Brain Extracellular Currents. Nauka, Moscow (in Russian).

Gutman, A. 1984. Nerve Cell Dendrites. Theory, Electrophysiology, Function. Mokslas, Vilnius, Lithuania (in Russian).

Gutman, A., and G. Svirskis. 1995. Theoretical analysis of DC field-induced polarization of ohmic neuron. *Biophysics.* 40:635–641 (translation from *Biofizika*).

Hounsgaard, J., and O. Kiehn. 1993. Calcium spikes and calcium plateaux evoked by differential polarization in dendrites of turtle motoneurones in vitro. *J. Physiol. (Lond.).* 468:245–259.

Hounsgaard, J., O. Kiehn, and I. Mintz. 1988. Response properties of motoneurones in a slice preparation of the turtle spinal cord. *J. Physiol. (Lond.).* 398:575–589.

Hounsgaard, J., and O. Kjaerulff. 1992. Ca^{2+}-mediated plateau potentials in a subpopulation of interneurons in the ventral horn of the turtle spinal cord. *Eur. J. Neurosci.* 4:183–188.

Jack, J. J. B., D. Noble, and R. W. Tsien. 1975. Electrical Current Flow in Excitable Cells. Clarendon Press, Oxford.

Jackson, M. B. 1992. Cable analysis with the whole-cell patch clamp. Theory and experiment. *Biophys. J.* 61:756–766.

Johnston, D., and S. M-S. Wu. 1995. Foundations of Cellular Neurophysiology. MIT Press, Cambridge, MA.

Kawato, M. 1984. Cable properties of a neuron model with non-uniform membrane resistivity. *J. Theor. Biol.* 111:149–169.

Larkman, A. U., G. Major, K. J. Stratford, and J. J. B. Jack. 1992. Dendritic morphology of pyramidal neurones of the visual cortex of the rat. IV. Electrical geometry. *J. Comp. Neurol.* 323:137–152.

Major, G. 1993. Solutions for transients in arbitrarily branching cables. III. Voltage clamp problems. *Biophys. J.* 65:469–491.

Major, G., J. D. Evans, and J. J. B. Jack. 1993. Solutions for transients in arbitrarily branching cables. I. Voltage recording with a somatic shunt. *Biophys. J.* 65:423–449.

Major, G., A. U. Larkman, P. Jonas, B. Sakmann, and J. J. B. Jack. 1994. Detailed passive cable models of whole-cell recorded CA3 pyramidal neurons in rat hippocampal slices. *J. Neurosci.* 14:4613–4638.

Okada, Y. C., J. C. Huang, M. E. Rice, D. Tranchina, and C. Nicholson. 1994. Origin of the apparent tissue conductivity in the molecular and granular layers of the *in vitro* turtle cerebellum and the interpretation of current source-density analysis. *J. Neurophysiol.* 72:742–753.

Rall, W. 1967. Distinguishing theoretical synaptic potentials computed for different soma-dendritic distributions of synaptic input. *J. Neurophysiol.* 30:1138–1168.

Rall, W., R. E. Burke, W. R. Holmes, J. J. B. Jack, S. J. Redman, and I. Segev. 1992. Matching dendritic neuron models to experimental data. *Physiol. Rev.* 72(Suppl.):S159–S186.

Rapp, M., I. Segev, and Y. Yarom. 1994. Physiology, morphology and detailed passive models of guinea-pig cerebellar Purkinje cells. *J. Physiol. (Lond.).* 474:101–118.

Richardson, T. L., and C. N. O'Reilly. 1995. Epileptiform activity in the dentate gyrus during low-calcium perfusion and exposure to transient electric fields. *J. Neurophysiol.* 74:388–399.

Ruigrok, T. J. H., A. Crowe, and H. J. Ten Donkelaar. 1984. Morphology of lumbar motoneurons innervating hindlimb muscles in the turtle *Pseudemys scripta elegans:* an intracellular horseradish peroxidase study. *J. Comp. Neurol.* 230:413–425.

Ruigrok, T. J. H., A. Crowe, and H. J. Ten Donkellar. 1985. Dendrite distribution of identified motoneurons in the lumbar spinal cord of the turtle *Pseudemys scripta elegans. J. Comp. Neurol.* 238:275–285.

Spielmann, J. M., Y. Laouris, M. A. Nordstrom, G. A. Robinson, R. M. Reinking, and D. G. Stuart. 1993. Adaptation of cat motoneurons to sustained and intermittent extracellular activation. *J. Physiol. (Lond.).* 464:75–120.

Spruston, N., D. B. Jaffe, and D. Johnston. 1994. Dendritic attenuation of synaptic potentials and currents: the role of passive membrane properties. *Trends Neurosci.* 17:161–166.

Svirskis, G., A. Gutman, and J. Hounsgaard. 1997. Detection of a membrane shunt by DC field polarisation during intracellular and whole-cell recording. *J. Neurophysiol.* 77:579–586.

Thurbon, D., A. Field, and S. Redman. 1994. Electrotonic profiles of interneurons in stratum pyramidale of the CA1 region of rat hippocampus. *J. Neurophysiol.* 71:1948–1958.

Tranchina, D., and C. Nicholson. 1986. A model for the polarization of neurons by extrinsically applied electric fields. *Biophys. J.* 50: 1139–1156.

Trifonov, Yu. A., and L. M. Chailakhian. 1975. Uniformed polarization of fibres and syncytial structures with extracellular electrodes. *Biofizika.* 20:107–112 (in Russian).

Turner, D. A., and P. A. Schwartzkroin. 1984. Passive electrotonic structure and dendritic properties of hippocampal neurons. *In* Brain Slices. R. Dingledine, editor. Plenum Press, New York and London. 25–50.